Electronic Supplementary Material (ESI) for Nanoscale.
This journal is © The Royal Society of Chemistry 2017

Electronic Supplementary Information (ESI)

High-Efficiency Near-Infrared enabled Planar Perovskite Solar Cells by Embedding Upconversion Nanocrystals

Fan-Li Meng [a], Jiao-Jiao Wu [a], Er-Fei Zhao [a], Yan-Zhen Zheng [a, b, *], Mei-Lan Huang [c], Li-Ming Dai [d], Xia Tao [a, b, *], Jian-Feng Chen [b]

[a] State Key Laboratory of Organic-Inorganic Composites, Beijing University of Chemical Technology, 15 Beisanhuan East Road, Beijing, 100029, P. R. China

[b] Research Center of the Ministry of Education for High Gravity Engineering & Technology, Beijing University of Chemical Technology, Beijing 100029, China, Email: zhengyz@mail.buct.edu.cn; chenjf@mail.buct.edu.cn

[c] School of Chemistry & Chemical Engineering, Queen's University Belfast, 10900 Euclid Avenue, Cleveland, OH44106, United Kingdom, Email: m.huang@qub.ac.uk

[d] Department of Macromolecular Science and Engineering

Case School of Engineering, Case Western Reserve University

10900 Euclid Avenue, Cleveland, OH44106, USA, Email: liming.dai@case.edu

* Corresponding author. Tel: +86-10-6445-3680 Fax: +86-10-6443-4784

E-mail: taoxia@yahoo.com (X. T.)

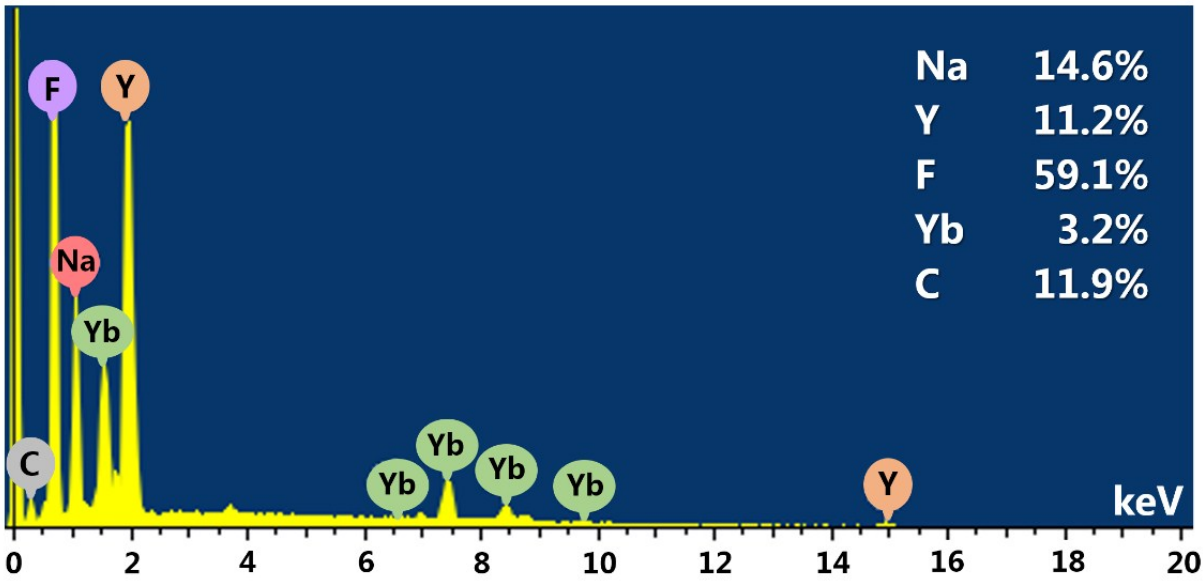

Fig. S1 EDS analysis of as-synthesized OM-capped β-$NaYF_4$:Yb,Er UCNCs.

Fig. S2 Photographs of the ligand-exchange process and the corresponding pictures before, during, and after ligand-exchange treatment, respectively.

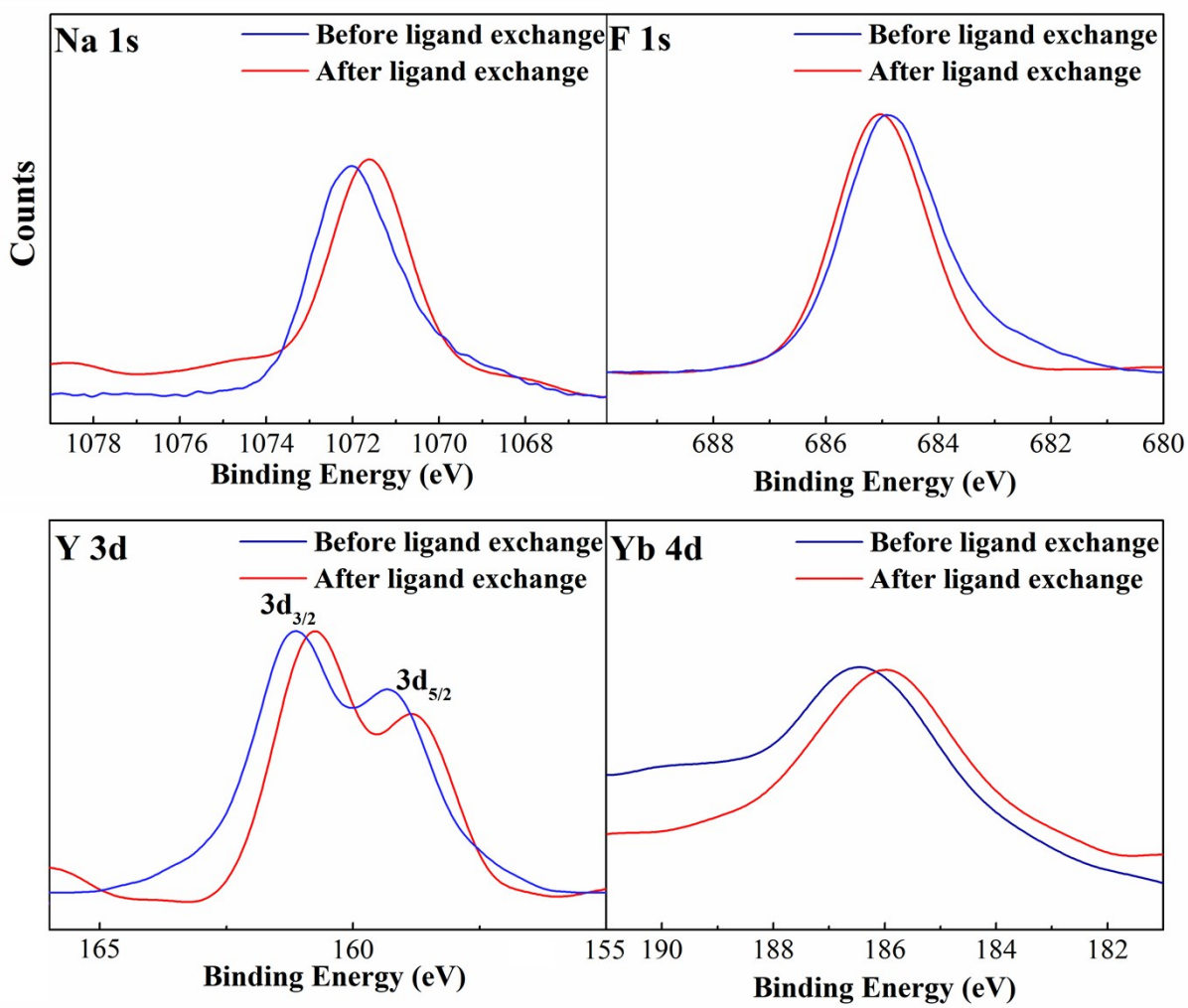

Fig. S3 XPS analysis of each individual element (N *1s*, I *3d*, Na *1s*, Y *3d*, F *1s*, and Yb *4d*) in the UCNCs before and after ligand-exchange treatment.

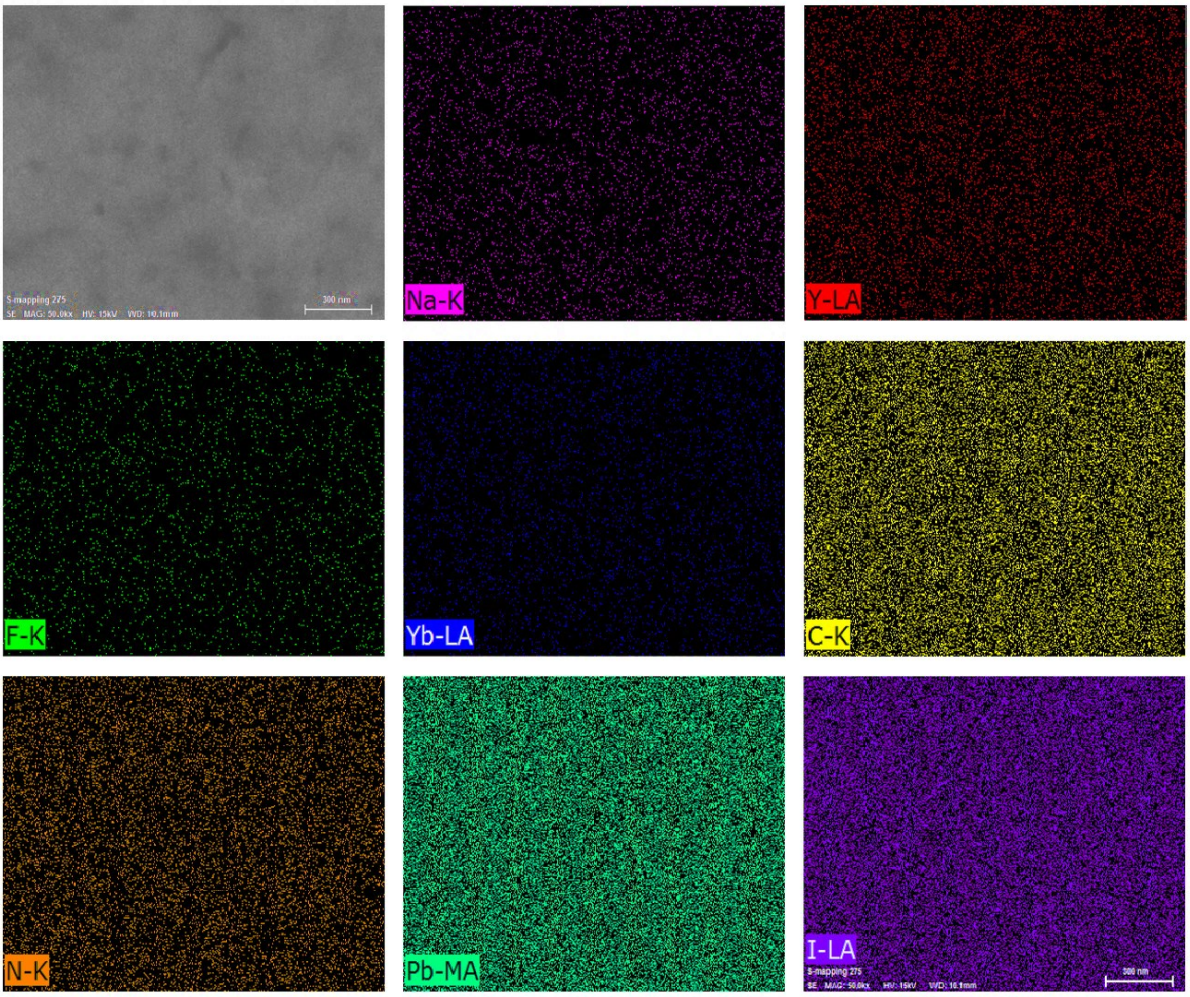

Fig. S4 SEM-EDS mapping images of UCNCs-embedded perovskite film.

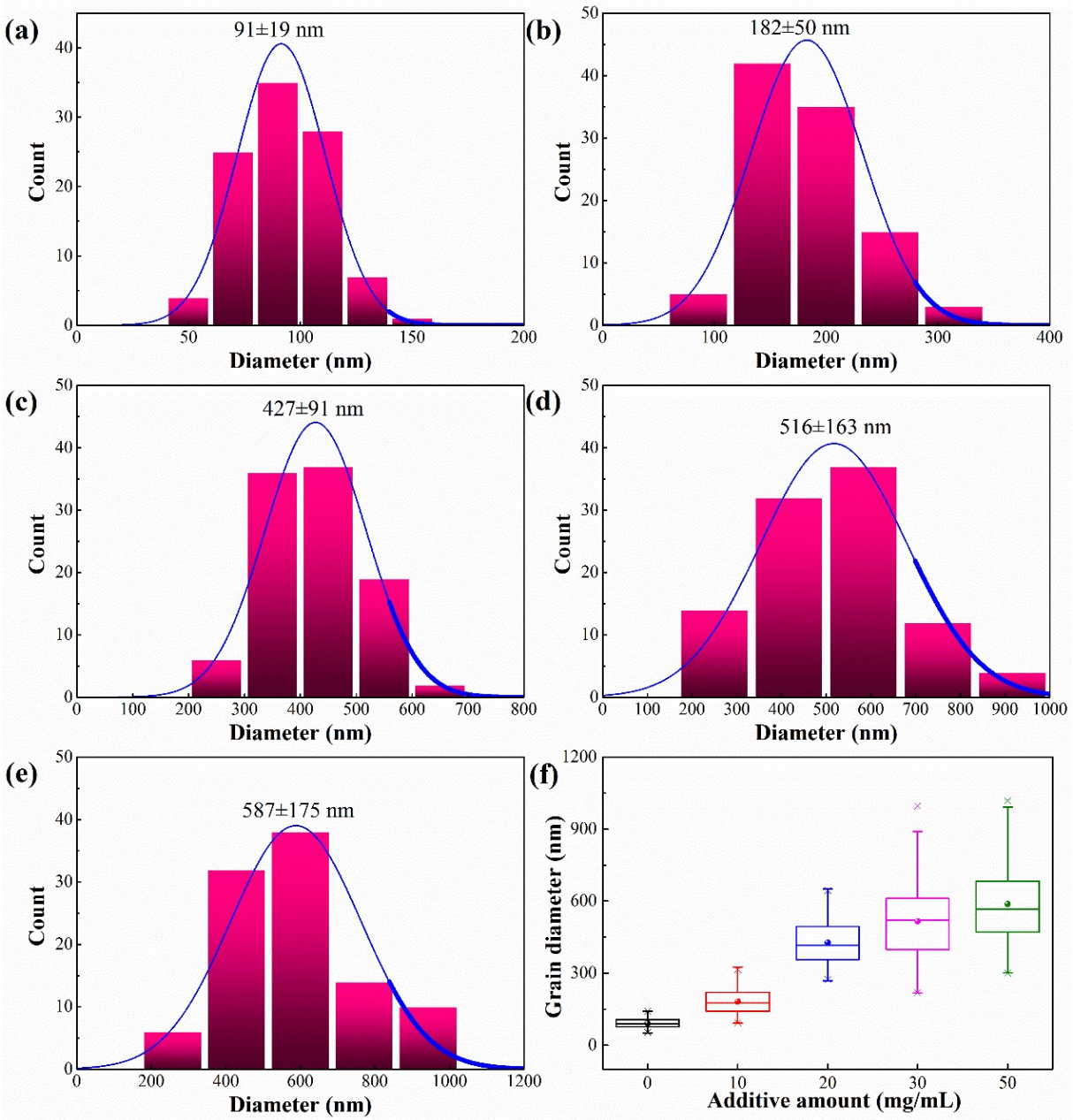

Fig. S5 Grain-size distribution results estimated from analysis of 100 grains for perovskite films with different amount of MAI-capped UCNCs. The results in (a–e) are corresponding to pristine, UC-10, UC-20, UC-30, and UC-50 samples, respectively. The average grain diameter ($\overline{d}$) is calculated from the Gaussian fit to the distribution. (f) The box chart of the variation as a function of $\overline{d}$ MAI-UCNCs additive amounts.

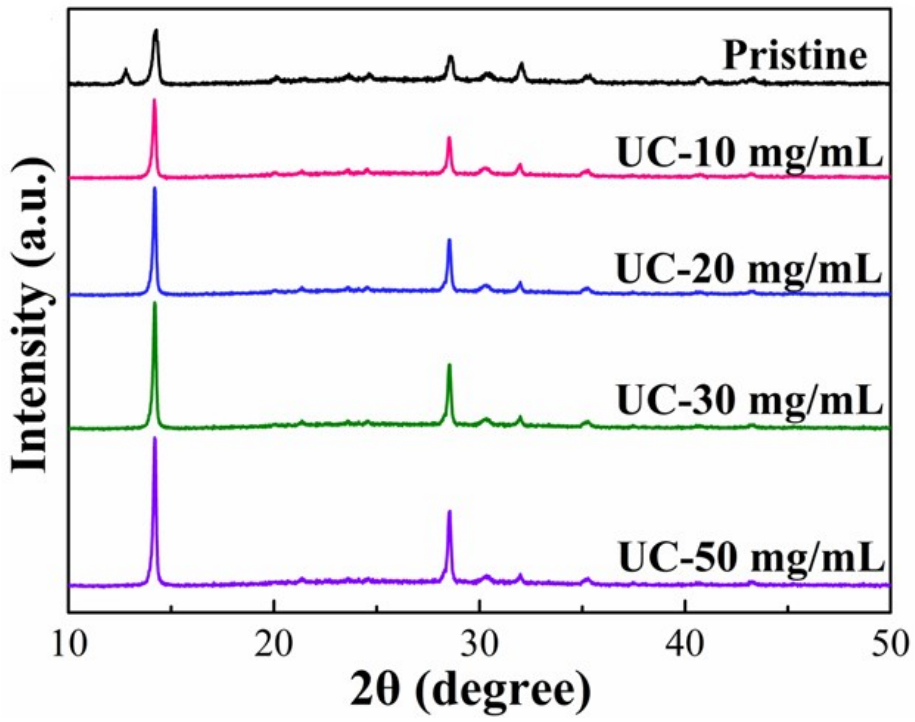

Fig. S6 XRD patterns of UCNCs-embedded perovskite films with different MAI-UCNCs additive amounts.

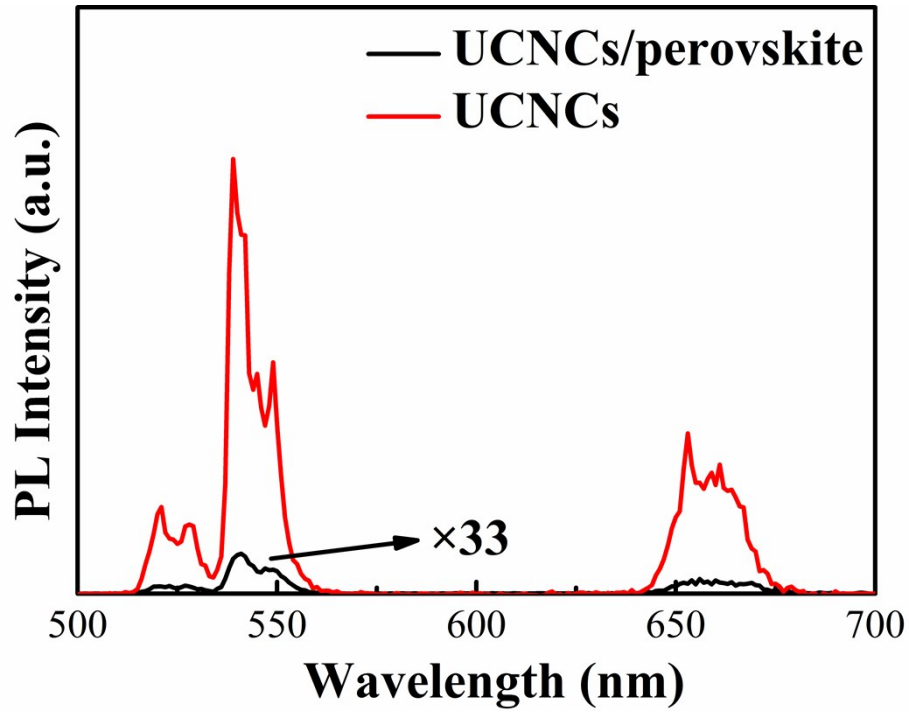

Fig. S7 Upconversion emission of as-synthesized UCNCs and UCNCs/perovskite powder obtained from UC-20 perovskite film with a UCNCs mass ratio of 3%. Note that the emission intensity from the UCNCs sample is multiplied by a factor of 33 in order to equivalently compare with the UCNCs/perovskite sample.

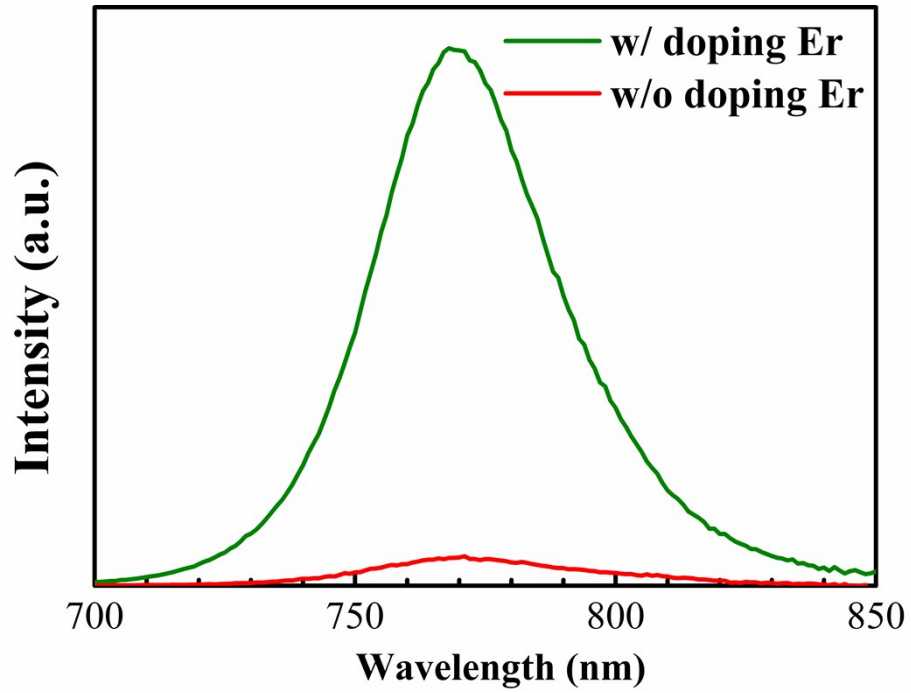

Fig. S8 Steady-state PL spectra of the perovskite films embedding with β-$NaYF_4$:Yb,Er and β-$NaYF_4$:Yb nanocrystals under the excitation of 980 nm laser.

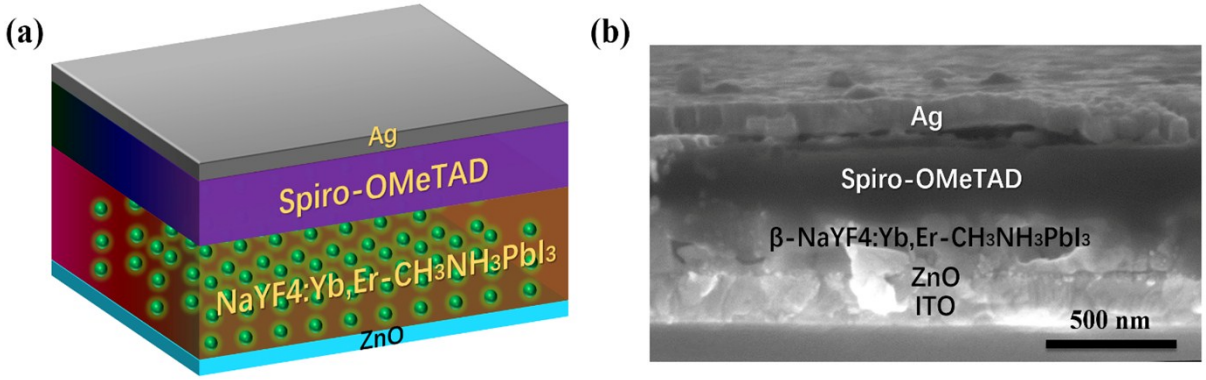

Fig. S9 (a) Schematic configuration and (b) cross-sectional SEM image of a complete UCNCs-embedded planar PSC device.

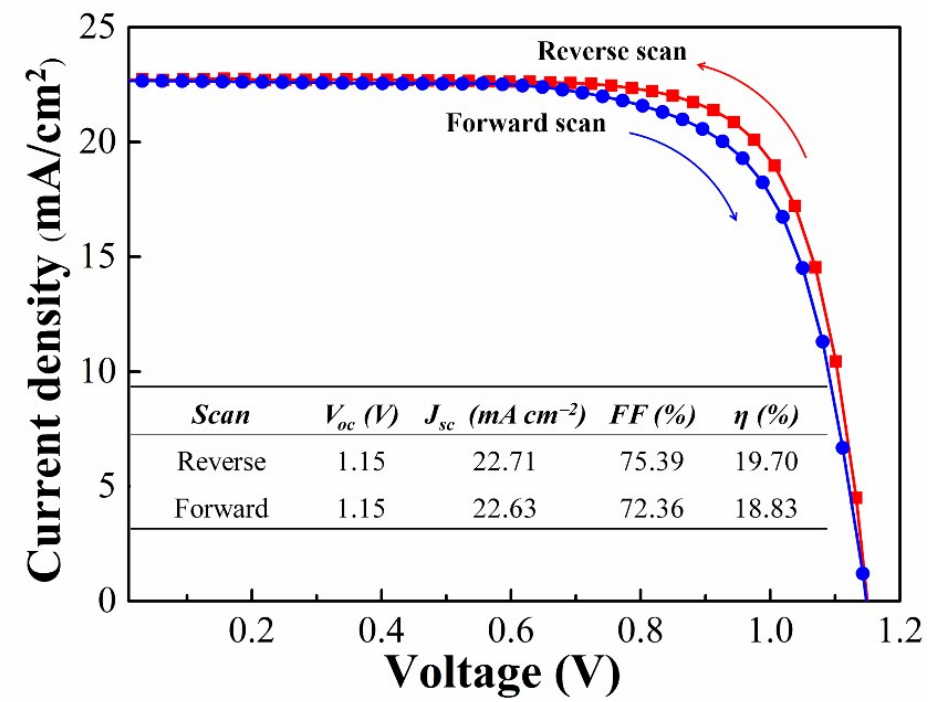

Fig. S10 Hysteresis characteristics of UC-20 planar PSC under AM 1.5G.

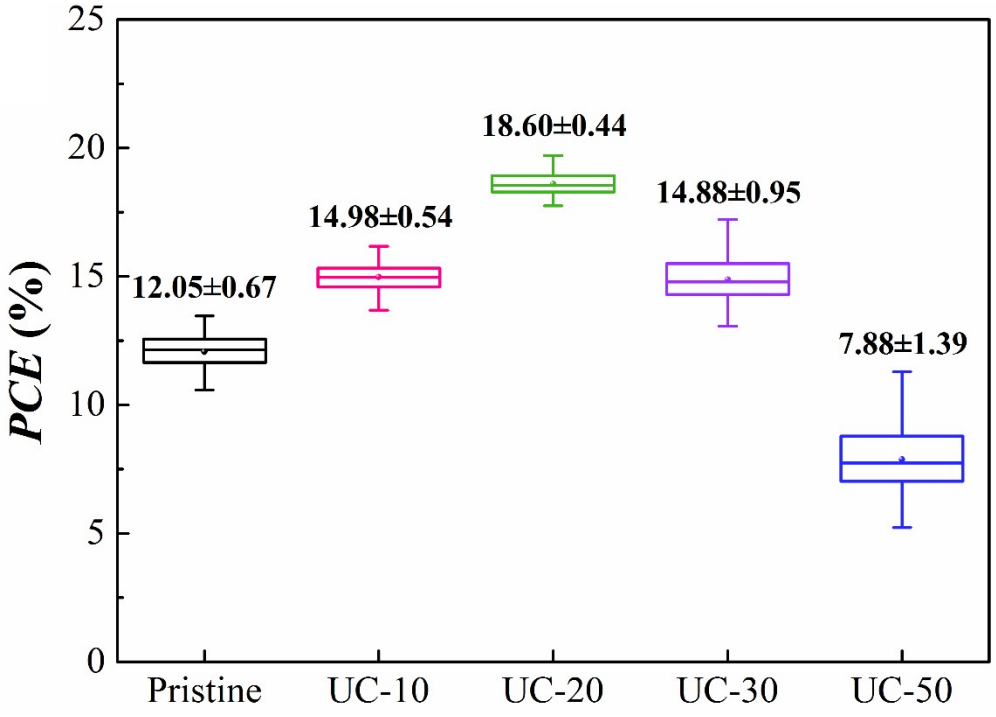

Fig. S11 Variation box chart of η for planar PSCs with different UCNCs additive amounts.

Table S1 Photovoltaic parameters of 50 individual pristine and UC-20 devices.

Device #	**Pristine**				**UC-20**			
	V_{oc} (V)	J_{sc} (mA cm^{-2})	*FF* (%)	*PCE* (%)	V_{oc} (V)	J_{sc} (mA cm^{-2})	*FF* (%)	*PCE* (%)
1	1.13	18.65	63.93	13.46	1.15	22.71	75.39	19.70
2	1.12	18.68	63.84	13.36	1.14	22.82	74.95	19.50
3	1.14	18.15	64.25	13.29	1.13	22.78	75.20	19.35
4	1.13	17.96	63.85	12.96	1.14	22.60	74.96	19.31
5	1.14	17.76	63.64	12.88	1.13	22.33	76.02	19.19
6	1.14	17.84	62.95	12.80	1.13	22.46	75.32	19.11
7	1.13	17.82	63.02	12.69	1.14	22.15	75.66	19.10
8	1.13	17.52	64.05	12.68	1.13	22.75	74.28	19.09
9	1.12	17.83	63.45	12.67	1.12	22.31	76.32	19.07
10	1.13	17.78	62.88	12.63	1.14	22.07	75.66	19.03
11	1.13	17.76	62.79	12.60	1.13	22.05	76.17	18.98
12	1.14	17.60	62.70	12.58	1.13	22.29	75.35	18.97
13	1.13	17.48	63.61	12.57	1.15	21.98	74.86	18.93
14	1.13	17.22	64.32	12.52	1.14	21.96	75.53	18.90
15	1.13	17.32	63.65	12.45	1.13	22.01	75.51	18.78
16	1.13	17.20	63.74	12.39	1.13	22.52	73.75	18.77
17	1.13	16.90	64.36	12.29	1.14	21.87	75.20	18.75
18	1.14	16.69	64.30	12.23	1.14	21.51	76.20	18.69
19	1.13	16.79	64.42	12.22	1.12	21.83	76.32	18.66
20	1.13	17.01	63.56	12.22	1.13	21.79	75.65	18.63
21	1.14	16.52	64.71	12.19	1.14	21.51	75.96	18.63
22	1.13	16.81	64.13	12.18	1.13	21.61	76.21	18.61
23	1.13	16.81	64.11	12.18	1.15	21.32	75.85	18.59
24	1.13	16.89	63.75	12.17	1.14	21.53	75.60	18.56
25	1.14	16.66	63.99	12.16	1.13	21.79	75.33	18.55
26	1.13	16.74	64.20	12.15	1.14	21.35	76.21	18.55
27	1.14	16.92	62.86	12.13	1.13	21.44	76.52	18.54
28	1.13	16.54	64.52	12.06	1.13	21.60	75.88	18.52
29	1.13	16.70	63.66	12.01	1.14	21.46	75.61	18.50
30	1.14	16.43	63.70	11.93	1.14	21.54	75.32	18.50

31	1.13	16.41	64.22	11.91	1.13	21.70	75.43	18.50
32	1.12	16.33	65.01	11.89	1.13	21.72	75.36	18.49
33	1.14	16.25	63.94	11.85	1.14	21.31	75.77	18.41
34	1.13	16.06	65.24	11.84	1.13	21.26	76.50	18.38
35	1.13	16.26	64.31	11.81	1.13	21.22	76.54	18.35
36	1.13	16.23	63.87	11.72	1.14	21.65	74.35	18.35
37	1.14	16.03	64.11	11.72	1.13	21.18	76.54	18.32
38	1.15	15.75	64.32	11.65	1.13	21.37	75.73	18.29
39	1.13	16.12	63.02	11.48	1.14	21.03	76.30	18.29
40	1.13	15.77	64.27	11.45	1.13	21.01	77.00	18.28
41	1.13	15.86	63.44	11.37	1.14	21.18	75.69	18.27
42	1.12	15.54	65.27	11.36	1.12	21.31	76.44	18.24
43	1.13	15.70	63.85	11.33	1.13	21.22	75.95	18.21
44	1.14	15.50	63.96	11.30	1.13	21.13	76.01	18.15
45	1.13	15.51	64.23	11.25	1.14	20.94	75.64	18.06
46	1.13	15.40	64.54	11.23	1.14	20.86	75.67	18.00
47	1.14	14.95	64.55	11.00	1.13	20.73	76.51	17.93
48	1.13	14.81	64.81	10.85	1.14	20.70	75.66	17.85
49	1.14	14.34	65.10	10.64	1.15	20.49	75.40	17.77
50	1.13	14.45	64.72	10.57	1.13	20.67	75.98	17.75

Table S2 Fit results of the TR-PL spectra in Fig. 3d. The decay curves were fitted with a tri-exponential function as PL intensity = $A + \Sigma B_i \exp(-t/\tau_i)$, and the relative content (Rel_i) of each lifetime constant (τ_i) was calculated by $Rel_i = B_i\tau_i/(\Sigma B_i\tau_i)$. The average PL lifetime constants ($\bar{\tau}$) are calculated by $\bar{\tau} = Rel_1\tau_1 + Rel_2\tau_2 + Rel_3\tau_3$.

Sample	τ_1 **(ns)**	Rel_1 **(%)**	τ_2 **(ns)**	Rel_2 **(%)**	τ_3 **(ns)**	Rel_3 **(%)**	$\bar{\tau}\ (ns)$
Pristine/SiO_2	3.73	0.37	45.24	6.26	144.83	93.37	138.07
UC-20/SiO_2	4.20	1.25	56.77	8.35	195.32	90.40	181.36
Pristine/ZnO	3.33	8.43	12.71	58.82	43.74	32.75	22.08
UC-20/ZnO	1.85	12.15	7.44	56.01	32.65	31.84	14.79

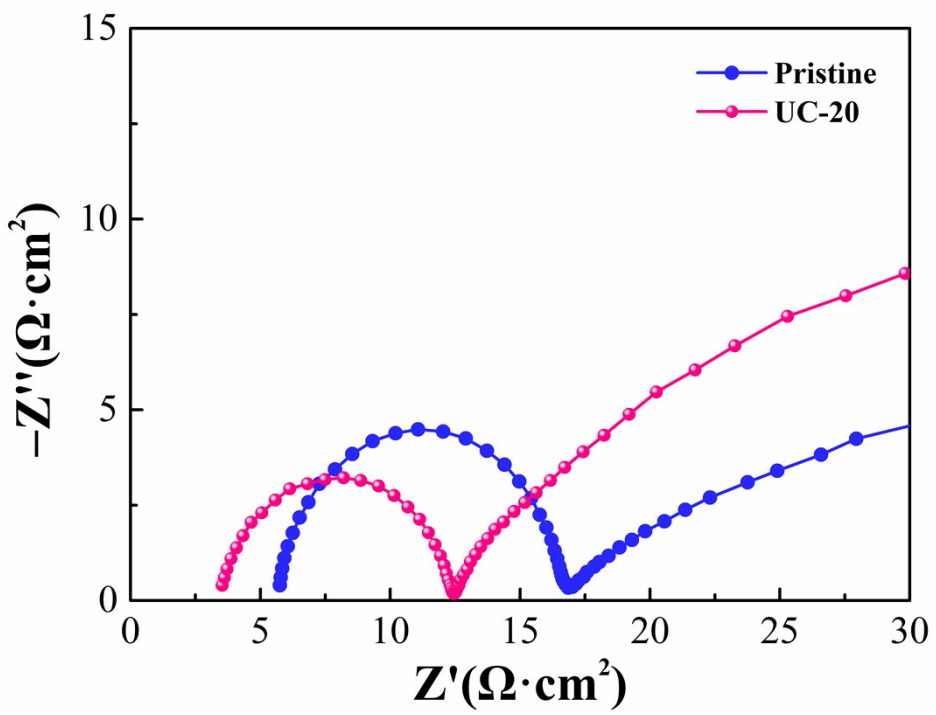

Fig. S12 EIS Nyquist plots of the pristine and UC-20 planar PSCs.

Table S3 Reported η of upconversion materials embedded PSC measured under 980 nm laser irradiation.

Device architecture	Upconversion materials	Particle size	Irradiance	η	Ref.
Mesoporous	β-$NaYF_4$:Yb,Er nanoprism	550–600 nm	11.1 W cm^{-2}	0.01%	1
Mesoporous	β-$NaYF_4$:Yb,Er nanoparticle	16.3±0.8 nm	28 W cm^{-2}	0.35%	2
Mesoporous	β-$NaYF_4$:Yb,Tm@$NaYF_4$ nanoparticle	45–50 nm	7.1 W cm^{-2}	0.083%	3

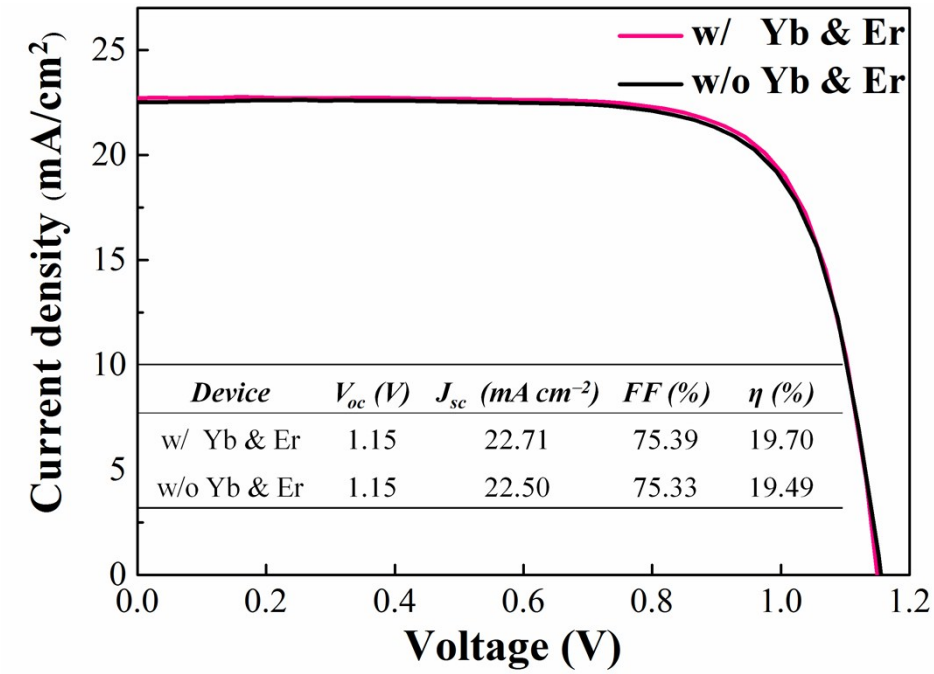

Fig. S13 *J–V* curves measured under AM 1.5G for β-$NaYF_4$:Yb,Er NCs-embedded PSC (w/ Yb & Er) and the β-$NaYF_4$ NCs-embedded PSC (w/o Yb & Er).

References

1. J. Roh, H. Yu and J. Jang, *ACS Appl. Mater. Interfaces*, 2016, **8**, 19847-19852.
2. M. He, X. Pang, X. Liu, B. Jiang, Y. He, H. Snaith and Z. Lin, *Angew. Chem. Int. Ed.*, 2016, **55**, 4280–4284.
3. M. Que, W. Que, X. Yin, P. Chen, Y. Yang, J. Hu, B. Yu and Y. Du, *Nanoscale*, 2016, **8**, 14432-14437.